Journal of Biomolecular NMR, 3 (1993) 165–184
ESCOM

J-Bio NMR 106

Sequence–specific ^{1}H and ^{15}N resonance assignments and secondary structure of GDP-bound human c-Ha-Ras protein in solution

Yutaka Muto[a], Kazuhiko Yamasaki[a], Yutaka Ito[a], Shunsuke Yajima[b], Haruhiko Masaki[b], Takeshi Uozumi[b], Markus Wälchli[c], Susumu Nishimura[d,*], Tatsuo Miyazawa[e] and Shigeyuki Yokoyama[a,**]

[a]*Department of Biophysics and Biochemistry, Faculty of Science, University of Tokyo, Hongo, Bunkyo-ku, Tokyo 113, Japan*
[b]*Department of Biotechnology, Faculty of Agriculture, University of Tokyo, Hongo, Bunkyo-ku, Tokyo 113, Japan*
[c]*Bruker Japan, Ninomiya, Tsukuba, Ibaraki 305, Japan*
[d]*National Cancer Center Research Institute, Tsukiji, Chuo-ku, Tokyo 104, Japan*
[e]*Protein Engineering Research Institute, Furuedai, Suita, Osaka 565, Japan*

Received 7 August 1992
Accepted 21 November 1992

Keywords: GTP binding protein; Oncogene product; Multi-dimensional NMR spectroscopy; Stable isotope labeling

SUMMARY

All the backbone ^{1}H and ^{15}N magnetic resonances (except for Pro residues) of the GDP-bound form of a truncated human c-Ha-*ras* proto-oncogene product (171 amino acid residues, the Ras protein) were assigned by ^{15}N-edited two-dimensional NMR experiments on selectively ^{15}N-labeled Ras proteins in combination with three-dimensional NMR experiments on the uniformly ^{15}N-labeled protein. The sequence-specific assignments were made on the basis of the nuclear Overhauser effect (NOE) connectivities of amide protons with preceding amide and/or C^{α}protons. In addition to sequential NOEs, vicinal spin coupling constants for amide protons and C^{α} protons and deuterium exchange rates of amide protons were used to characterize the secondary structure of the GDP-bound Ras protein; six β strands and five helices were identified and the topology of these elements was determined. The secondary structure of the Ras protein in solution was mainly consistent with that in crystal as determined by X-ray analyses. The deuterium exchange rates of amide protons were examined to elucidate the dynamic properties of the secondary structure elements of the Ras protein in solution. In solution, the β-sheet structure in the Ras protein is rigid, while the second helix (A66–R73) is much more flexible, and the first and fifth helices (S17–124 and V152–L171) are more rigid than other helices. Secondary structure elements at or near the ends of the effector-region loop were found to be much more flexible in solution than in the crystalline state.

*Present address: Banyu Tsukuba Research Institute in Collaboration with Merck Sharp and Dohme Research Laboratories, Banyu Pharmaceutical Co. Ltd., Tsukuba Techno-Park Oho, Okubo 3, Tsukuba 300–33, Japan.
**To whom correspondence should be addressed.

0925-2738/$ 10.00 © 1993 ESCOM Science Publishers B.V.

INTRODUCTION

The human c-Ha-*ras* gene (Krontiris and Cooper, 1981; Perucho et al., 1981; Shih et al., 1981) is a member of the *ras* proto-oncogene family involved in certain processes of cell proliferation and differentiation. The product of this gene, the Ras protein, which consists of 189 amino acid residues, is tightly bound to GDP or GTP (Barbacid, 1987; Nishimura and Sekiya, 1987). The GDP-bound Ras protein is predominant in non-stimulated cells, whereas the GTP-bound Ras protein is present in increased amounts in cells stimulated by proliferation or differentiation signals (Barbacid, 1987; Satoh et al. 1987, 1990a,b, 1991; Trahey and McCormick, 1987). In this context, 'exchange factors' which accelerate the dissociation of GDP from the Ras protein have been found (Downward et al., 1990; West et al., 1990; Wolfman and Macara, 1990; Mizuno et al., 1991). The GDP-bound Ras protein probably receives the signal by interacting with an 'exchange factor' upstream in the signal-transduction pathway, which results in the formation of the GTP-bound Ras protein (Barbacid, 1987; Satoh et al., 1987, 1990a,b, 1991). In turn, the GTP-bound Ras protein interacts with a putative effector, which transduces the signal further (Barbacid, 1987; Satoh et al., 1987; Trahey and McCormick, 1987; Satoh et al., 1991). The Ras protein itself has GTPase activity, by which the GTP-bound form is converted back to the GDP-bound form and can receive the signals again (Barbacid, 1987).

The conformation of the Ras protein in aqueous solution has been studied mainly by NMR spectroscopy (Schlichting et al., 1988, 1990b; Campbell-Burk, 1989; Campbell-Burk et al., 1989; Ha et al., 1989; Hata-Tanaka et al., 1989; Yamasaki et al., 1989; Redfield and Papastavros, 1990; Fujita-Yoshigaki et al., Miller et al., 1992; Yamasaki et al., 1992). For human N-Ras protein, selective ^{15}N-labeling techniques have been applied for Gly and Lys residues, and selective ^{13}C–^{15}N labeling techniques (Kainosho and Tsuji, 1982) have been used for partial resonance assignments (Campbell-Burk, 1989; Campbell-Burk et al., 1989; Redfield and Papastavros, 1990). Circular dichroic spectroscopy (Pingoud et al., 1988; Valencia et al., 1988) and fluorescence spectroscopy (John et al., 1990; Neal et al., 1990; Skelly et al., 1990; Antonny et al., 1991; Rensland et al., 1991) have also been applied to the Ras protein. However, the overall conformation of the Ras protein in solution is yet to be elucidated.

A 'truncated Ras protein' lacking the C-terminal 18 amino acid residues [Ras(1–171) protein] has the same GTP/GDP binding and GTPase activities as those of the full-length Ras protein (Ha et al., 1989; Fujita-Yoshigaki et al., 1992). Furthermore, the conformation of the Ras(1–171) protein is nearly the same as that of the corresponding region of the Ras protein (Ha et al., 1989; Fujita-Yoshigaki et al., 1992). The 3D structures of the Ras(1–171) proteins in the GDP-bound form (de Vos et al., 1988; Tong et al., 1989, 1991) and of the Ras(1–166) and Ras(1–171) proteins in the GTP-bound form (Pai et al., 1989, 1990; Brünger et al., 1990; Milburn, et al., 1990) have been determined by X-ray crystallography. Further, the tertiary structures of the truncated form

---

Abbreviations: Asx, Asp and/or Asn; COSY, two-dimensional correlation spectroscopy; DQF-COSY, double-quantum filtered COSY; DSS, sodium 2,2-dimethyl-2-silapentane-5-sulfonate; Glx, Glu and/or Gln; GTPase, guanosine 5'-triphosphatase; HMQC, heteronuclear multiple-quantum coherence; HSQC, heteronuclear single-quantum coherence; HTQC, heteronuclear triple-quantum coherence; NOESY, two-dimensional nuclear Overhauser effect spectroscopy; Ras (1–166) protein, a truncated Ras protein lacking the C-terminal 23 amino acid residues; Ras(1–171) protein, a truncated Ras protein lacking the C-terminal 18 amino acid residues; TOCSY, total correlation spectroscopy; TPPI, time proportional phase incrementation.

of the transforming mutant Ras proteins [Ras(1–171) or Ras(1–166)] have been compared with that of the normal Ras(1–171) or Ras(1–166) protein (Krengel et al., 1990; Tong et al., 1991; Privé et al., 1992). The conformation of the Ras(1–171) protein in aqueous solution has also been studied by NMR (Ha et al., 1989; Hata-Tanaka et al., 1989; Yamasaki et al., 1989). The GDP-bound Ras(1–171) protein in solution has been shown to have a typical antiparallel β-sheet structure involving some functionally important residues (Yamasaki et al., 1989). However, the β-sheet structure is appreciably distorted around the important residues of the GTP-bound Ras(1–171) protein in solution (Yamasaki et al., 1989). These differences between the GDP-bound and GTP-bound forms has not been observed in the crystal structure (Milburn et al., 1990; Schlichting et al., 1990a).

Therefore, it is important to elucidate the solution structure of the Ras(1–171) protein further by using stable isotope-aided NMR techniques developed for proteins consisting of more than 100 amino acid residues (LeMaster and Richards, 1985, 1988; Torchia et al., 1988, 1989; Muchmore et al., 1989; Bax et al., 1990a–c; Ikura et al., 1990b–d, 1991; Kay and Bax, 1990; McIntosh and Dahlquist, 1990; McIntosh et al., 1990; Bax and Ikura, 1991). Note that there are only a few reports for proteins consisting of more than about 170 amino acids (Stockman et al., 1990, 1992; Clubb et al., 1991; Pelton et al., 1991). For Ras(1–171) protein, we have already selectively labeled 15 amino acid types with ^{15}N to classify resonances in HMQC/ HSQC spectra (Yamasaki et al., 1992).

In the present study, the GDP-bound Ras(1–171) protein was analyzed further by proton-detected heteronuclear magnetic resonance experiments with selective ^{15}N-labeling for specific amino acid types and uniform ^{15}N-labeling. Thus, all the backbone ^{1}H and ^{15}N resonances (except for Pro residues) were assigned completely and the secondary structures and dynamic properties of the protein in solution were elucidated.

MATERIALS AND METHODS

Preparation of the Ras protein

A gene coding for the Ras(1–171) protein (Ha et al., 1989) constructed from a synthetic full-length gene (Miura et al., 1986) was used to prepare the NMR samples. *Escherichia coli* strain TG1, transfected with a *trp*-promoter expression vector containing the truncated *ras* gene, was cultured, induced and harvested; 8 g of wet cells were collected from 2 l of 2 × M9 medium containing casamino acids. Purification of the Ras(1–171) protein was performed as described previously (Ha et al., 1989); 50–100 mg of the protein was obtained from 8 g of wet cells. Hereafter we refer to the Ras(1–171) protein as the Ras protein.

Preparation of uniformly ^{15}N-labeled Ras protein

Uniformly ^{15}N-labeled protein was prepared by replacement of $^{14}NH_4Cl$ with $^{15}NH_4Cl$ (Isotec Inc.) in 2 × M9 medium with 240 mg/l $MgSO_4$, 15 mg/l $CaCl_2$, 20 mg/l thiamine and 4 g/l glucose. $^{15}NH_4Cl$ was from Isotec Inc. Preculture (200 ml scale) in stationary phase was added to 4 l of culture medium and the cells were induced.

Preparation of selectively ^{15}N-labeled Ras proteins

Selective ^{15}N-labeling (McIntosh and Dahlquist, 1990; McIntosh et al., 1990) of the Ras protein

was performed by using auxotrophic *E. coli* strains which lack some transaminase activities (Yamasaki et al., 1992): a general transaminase-deficient strain DL39 (LeMaster and Richards, 1988) was used for selective labeling of Val, Leu, Ile, Ala, Phe, Tyr, and Asx (*aspC*, *avtA*, *ilvE*, *tyrB*), strain PC0950 (*thr*, *argF*, *argI*, *serB*, *purA*) for Gly, Ser and Thr, strain AB1255 (*hisG*, *argF*, *argI*, *argH*) for Arg, Met, and His, strain AT2457 (*glyA*) for Gly, strain PA340 (*gdh*, *gltB*) for Glx, and strain JE5811 (*lys*) for Lys. Strains DL39, PC0950, AB1255, AT2457 and PA340 were gifts from Dr. B.J. Bachmann of Yale University (Bachmann, 1983), and strain JE5811 was a gift from Dr. A. Nishimura of the National Institute of Genetics, Japan. These strains were grown in 2 × M9 medium containing 4 g/l disodium succinate, 4 g/l D,L-malate, 240 mg/l $MgSO_4$, 15 mg/l $CaCl_2$, and 20 mg/l thiamine. Preculture in stationary phase was added to culture medium containing one or two ^{15}N-labeled amino acids and other nonlabeled amino acids. ^{15}N-labeled amino acids were from ICON (Ala, Arg, Gly, Phe, Ser, Thr and Tyr), Isotec Inc. (Asp), CIL (Glu and Ile), VEB Berlin Chemie (Lys and Val), Commissariat à l'Energie Atomique (His) and Shoko Co., Ltd. (Met). ^{15}N-Labeled Ras proteins were purified as described for the nonlabeled Ras protein (Ha et al., 1989). Yields of the Ras proteins were estimated from the specific absorbance: $A_{280} = 0.56\ cm^{-1}\ mg^{-1}$ ml.

Preparation of NMR samples

For NMR measurements, 15 mg of the Ras protein was used. The solution of the Ras protein was mixed with 20 mM phosphate buffer (pH 5.5) containing 10 mM $MgCl_2$ and 150 mM NaCl. The protein solution was concentrated by ultrafiltration with a Centricon-10 or Centriprep-10 (Amicon). 99.85% ^2H_2O (Commissariat à l'Energie Atomique) was added to a concentration of 10% for lock stabilization. Final samples (0.18 ml) used for NMR measurements contained 50 mg/ml protein.

NMR measurements

Two-dimensional and 3D NMR spectra were recorded with Bruker AM-400 and/or AM-600 spectrometers at a probe temperature of 37°C. ^1H chemical shifts were determined relative to internal DSS, and ^{15}N chemical shifts were determined relative to the ^{15}N resonance of external $^{15}NH_4Cl$ in 1M HCl.

Two-dimensional ^1H–^{15}N NMR experiments

Heteronuclear HSQC (Bodenhausen and Ruben, 1980) and HMQC (Müller, 1979; Bax et al., 1983a,b; Bendall et al., 1983) spectra were measured with delays of 2.3 ms and 4.5 ms, respectively, rather than 2.7 ms ($1/4J_{NH}$) or 5.4 ms ($1/2J_{NH}$), to reduce the loss of coherence due to relaxation (Driscoll et al. 1990). The sweep width for ^1H was 6500 Hz, and that for ^{15}N was 2000 Hz. The GARP1 pulse sequence (Shaka et al. 1985) was used for ^{15}N decoupling during the ^1H-detected acquisition period. Free induction decays were collected with 2K data points in the t_2 domain, and 300–400 increments in the t_1 domain. For each t_1 value, 32–160 scans were accumulated. In order to obtain spectra in the phase-sensitive mode, the TPPI method (Marion and Wüthrich 1983) was used. The residual ^1H_2O and $^1H^2HO$ resonances were suppressed by selective presaturation. The data were processed with Gaussian resolution enhancement and zero-filling to 1K data points in the $F_1(^{15}N)$ dimension.

HMQC-COSY (Clore et al., 1988), HMQC-TOCSY and HSQC-NOESY (Gronenborn et al.,

1989; Bax et al., 1990c) spectra were made for the uniformly ^{15}N-labeled Ras protein. In the HMQC-TOCSY experiment, an MLEV17 pulse train (Bax and Davis, 1985) of 45 ms with a preceding trim pulse was used for mixing. In the HSQC-NOESY experiment, the mixing time was 100 ms. The HTQC spectra were acquired to identify $^{15}N^1H_2$ resonances in the HSQC spectra (Schmidt and Rüterjans, 1990). The acquisition and data processing conditions were the same as those for HSQC or HMQC measurements.

Two-dimensional ^1H NMR experiments

Phase-sensitive DQF-COSY (Rance et al., 1983; Shaka and Freeman, 1983), NOESY (Jeener et al., 1979; Kumar et al., 1980; Macura and Ernst, 1980) and TOCSY (Braunschweiler and Ernst, 1983; Davis and Bax, 1985) spectra were recorded of Ras proteins in ^1H_2O and ^2H_2O solutions with a sweep width of 6500 Hz. The water resonance was suppressed by selective preirradiation in DQF-COSY experiments. In addition to the preirradiation for water suppression, the last reading pulse was replaced by a jump-and-return pulse (Plateau and Gueron, 1982) in NOESY and TOCSY experiments (Bax et al., 1987; Driscoll et al. 1989). In TOCSY experiments, an MLEV17 pulse train of 45 ms (Bax and Davis, 1985) was used with a preceding trim pulse. Mixing times in NOESY measurements were in a range of 80–150 ms. All measurements were performed by the TPPI method to obtain phase-sensitive spectra. The data were collected with 2K data points in the t_2 domain and 360 increments in the t_1 domain and were transformed into 2K × 1K points after zero-filling for the t_1 domain to 1K points.

Two-dimensional isotope-edited ^1H NMR experiments

^{15}N-edited COSY and NOESY spectra of uniformly and selectively ^{15}N-labeled Ras proteins were recorded by replacing the final 90° pulse with a difference echo sequence (Otting et al., 1986; Fesik et al., 1987; Griffey and Redfield, 1987; McIntosh et al., 1990). Coherence transfer in TOCSY experiments was achieved with a WALZ16 mixing pulse train preceded by a 3-ms trim spin-locking pulse (Driscoll et al., 1989, 1990). In order to reduce the rotating frame NOE, this mixing pulse train was sandwiched by two 90°-proton pulses with a 5-ms delay (Driscoll et al., 1989, 1990). The sweep width was 6800 Hz in both dimensions. The data were collected as 360–400 t_1 increments by the TPPI method, and with 2K data points in the t_2 domain. Edited NOESY spectra were recorded with a mixing time of 100 ms. The processing of ^{15}N-edited NMR data was the same as for conventional 2D proton NMR spectra.

Three-dimensional NMR experiments

^1H–^{15}N heteronuclear NOESY-HMQC and TOCSY-HMQC spectra (Marion et al., 1989; Zuiderweg and Fesik, 1989) of uniformly ^{15}N-labeled Ras protein were recorded. The mixing times were 30 ms in TOCSY-HMQC and 100 ms in NOESY-HMQC experiments. For both experiments, sweep widths were 6800 Hz (F_1), 6800 Hz (F_2) and 2400 Hz (F_3, 40 ppm in the ^{15}N dimension). In TOCSY-HMQC experiments, the WALZ16 spin-locking pulse train was sandwiched by two 90°-pulses with 5-ms delays. Quadrature detection in the t_1 and t_2 domains was performed with the TPPI method. In each case, 128 real t_1, 64 real t_2, and 512 real t_3 data points were recorded. The 3D data were processed by multiplication by a squared-sine bell window function and zero-filling to yield the final absorption spectrum of 256(F_1) × 64(F_2) × 512(F_3) data points. The 3D HMQC-NOESY-HMQC spectrum (Ikura et al., 1990a) was recorded with a

mixing time of 100 ms and sweep widths were 4600 Hz (F_1), 1600 Hz (F_2) and 1600 Hz (F_3). The methods for data acquisition and processing were the same as described above.

Measurement of $^3J_{HNH\alpha}$ coupling constants

Accurate values of $^3J_{HNH\alpha}$ coupling constants were determined from HMQC-J spectra (Kay and Bax, 1990) and HSQC spectra were obtained with a novel DANTE water-suppression pulse train (Kay et al. 1989). The sweep width for the ^1H dimension was 3400 Hz and that for the ^{15}N dimension was 1600 Hz. A total of 4K data points for the t_2 domain and 1K t_1 increments were collected. After zero-filling in the t_1 time domain and application of a Gaussian window function for both the t_2 and t_1 domains, the digital resolution was 1.0 Hz/point in the F_1 domain. $^3J_{HNH\alpha}$ coupling constants were obtained from the splitting of cross peaks in the F_1 dimension by using the correction procedure described (Kay and Bax, 1990).

Measurements of deuterium exchange rates

To identify backbone amide protons involved in hydrogen bonds, the Ras protein in H_2O solution was lyophilized and dissolved in 99.98% ^2H_2O to allow deuterium exchange. After 5 min, a series of HSQC spectra were recorded for 24 h, each of which took about 1 h.

RESULTS AND DISCUSSION

^1H–^{15}N correlation spectrum of uniformly ^{15}N-labeled Ras protein

In our previous study (Yamasaki et al., 1992), the uniformly ^{15}N-labeled Ras protein preparation contained traces of protein impurities, but in the present study the preparation was purer. Thus, the sequence-specific assignment of all the backbone ^1H–^{15}N cross peaks of the GDP-bound Ras protein in solution was completed, as shown in the HSQC spectrum in Fig. 1. Because

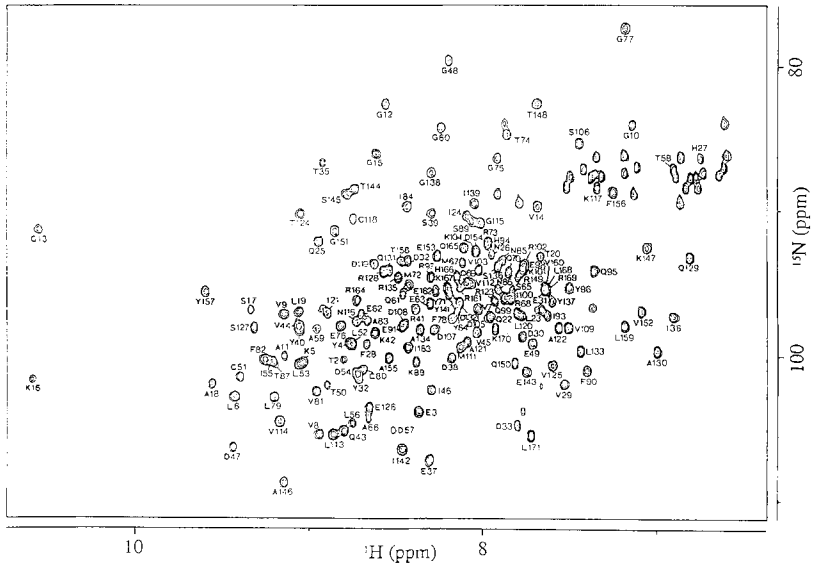

Fig. 1. Amide region of the HSQC spectrum of the uniformly ^{15}N-labeled Ras protein in ^1H_2O solution.

of the large number of residues, some cross peaks contain two to four overlapped peaks. Therefore, all the backbone amide ^{1}H–^{15}N cross peaks were classified into amino acid types on the basis of previous ^{1}H–^{15}N HSQC/HMQC spectra of the Ras proteins with selectively ^{15}N-labeled amino acid residues (Yamasaki et al., 1992).

Isotope-aided NOESY and TOCSY experiments

In order to identify d_{NN} and $d_{\alpha N}$ connectivities for sequential assignments (Wüthrich et al., 1984; Wüthrich, 1986), ^{15}N-edited NOESY, COSY and TOCSY spectra (Torchia et al., 1988, 1989; Muchmore et al., 1989; McIntosh and Dahlquist, 1990; McIntosh et al., 1990) were recorded for 14 preparations of Ras proteins with selectively ^{15}N-labeled residues (Leu, Val, Ile, Ala, Thr, Lys, Arg, Gly, Ser, Tyr, Phe, His, Asx, and Met) (Yamasaki et al., 1992). Further, 3D NOESY-HMQC and TOCSY-HMQC spectra (Marion et al., 1989; Zuiderweg and Fesik, 1989) were recorded for the uniformly ^{15}N-labeled Ras protein. By using these data, NOESY and TOCSY cross peaks of the Ras protein were assigned in relation to the ^{1}H–^{15}N cross peaks in the HSQC spectrum. Some details of the strategies will be explained below for typical cases.

Degeneracy of ^{1}H and ^{15}N chemical shifts in 3D NMR spectra

For complete sequential assignment of residues in the Ras protein, it was necessary to resolve the degeneracies in ^{1}H and ^{15}N chemical shifts. For example, in the HSQC spectrum (Fig. 1), the ^{1}H–^{15}N cross peak at δ (^{1}H) = 7.65 ppm and δ (^{15}N) = 95.3 ppm is a degenerate peak due to E31, V160, L168 and R169. However, in the HMQC spectrum of the Ras protein selectively labeled with [^{15}N]leucine (Fig. 2), the cross peaks due to the 13 Leu residues of Ras protein are clearly resolved from one another, exhibiting a single peak due to L168. Thus, in the ^{15}N-edited NOESY (Fig. 3) and TOCSY (data not shown) spectra of the Ras proteins selectively labeled with [^{15}N]leucine, [^{15}N]valine, and [^{15}N]arginine, cross peaks due to V160, L168 and R169 were identified separately. This method was not useful for identifying the cross peaks of E31, because selective labeling with [^{15}N]Glu was not efficient (to be discussed later).

Degeneracy of ^{1}H chemical shifts in ^{15}N-edited spectra

The amide proton resonances of L19 and L53 of the Ras protein selectively labeled with [^{15}N]leucine had the same chemical shift (9.05 ppm) in the HMQC spectrum (Fig. 2) and the ^{15}N-edited NOESY spectrum (Fig. 3). Therefore, we examined the 3D NOESY-HMQC and

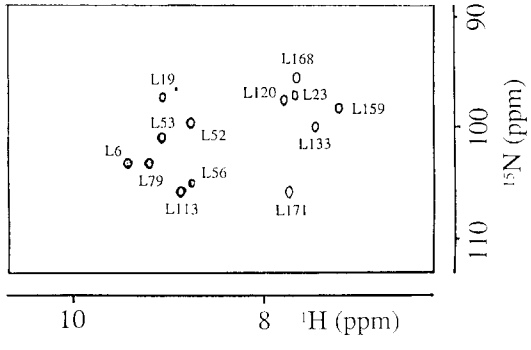

Fig. 2. Amide region of the HMQC spectrum of the Ras protein selectively labeled with [^{15}N]leucine.

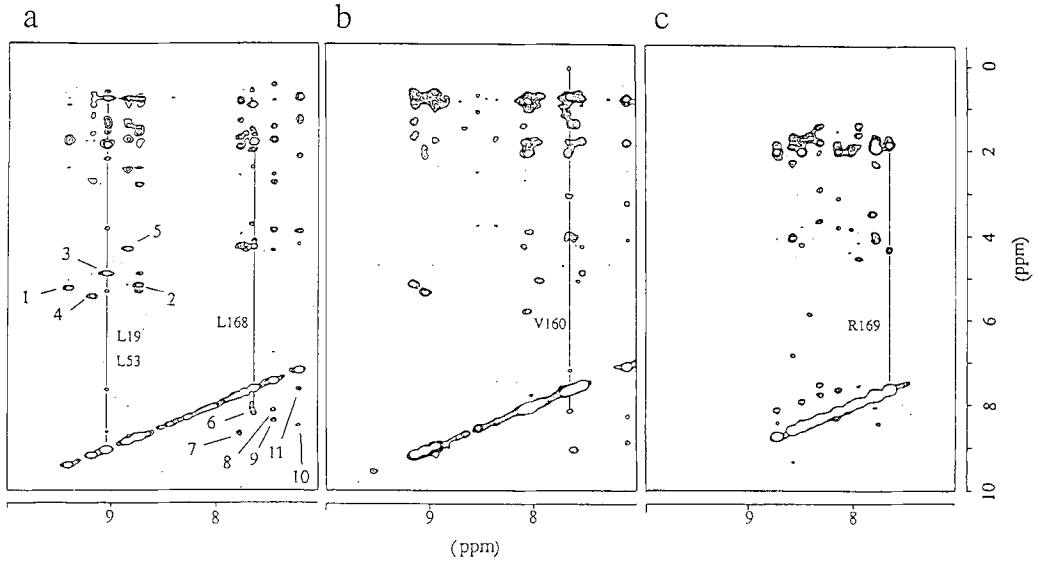

Fig. 3. ^{15}N-Edited NOESY spectra of Ras proteins selectively labeled with [^{15}N]leucine (a), [^{15}N]valine (b), and [^{15}N]arginine (c). Cross peaks due to L19, L53, L168, V160, and R169 are indicated by vertical lines. L19 and L53 have the same amide proton chemical shifts. In (a), the cross peaks for the amide and C_α protons are shown with 1: L6, 2: L52, 3: L53, 4: L79, and 5: L113. The cross peaks for pairs of amide protons are also shown with 6: Q22–L23, L23–I24, and K167–L168, 7: D119–L120, 8: D132–L133, 9: L133–A134, 10: T158–L159, and 11: L159–V160.

TOCSY-HMQC spectra as well as the 2D HMQC-NOESY, HMQC-TOCSY and HMQC-COSY spectra of the uniformly ^{15}N-labeled Ras protein. In fact, the NOE cross peaks due to L19 were clearly identified in a slice to the 3D NOESY-HMQC spectrum (Fig. 4a), and so were those due to L53 in another slice (data not shown). Thus, for Leu, Val, Ile, Lys, Arg, Gly, Ser, Met, His, Phe, Tyr, Asx, Ala and Thr residues, COSY, TOCSY and NOESY cross peaks due to each residue were identified almost completely by the combined use of selective and uniform ^{15}N-labeling techniques.

Identification of Glx resonances

^{15}N-Edited TOCSY, COSY and NOESY methods are not useful for identifying TOCSY/NOESY cross peaks due to Glx residues. However, the amide resonances of Glx residues were assigned in the HSQC experiment with the Ras protein selectively labeled with [^{15}N]Glx, and the TOCSY and NOESY cross peaks due to those Glx residues were identified by 3D NMR techniques. For example, Figs. 4b and 4c show the slices of 3D NOESY-HMQC and TOCSY-HMQC spectra at δ (^{15}N) = 104.0 ppm, where the cross peaks due to E126 and E3 are unambiguously identified. Among the ^{1}H–^{15}N cross peaks of 24 Glx residues, those of E31 and E98 each overlap with others in the HSQC spectrum (Fig. 1), making identification of their NOE cross peaks impossible. For these two Glu residues, resonance assignments were finally achieved from sequential NOE(s) with the backbone protons of the preceding and/or succeeding residues (see below).

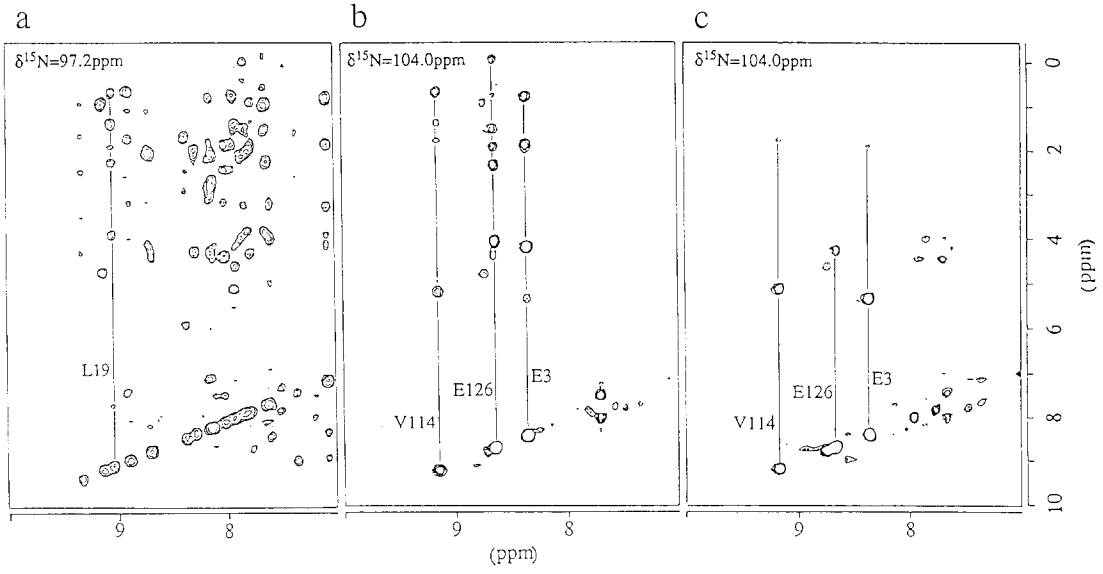

Fig. 4. Slices from the 3D NOESY-HMQC (a and b) and 3D TOCSY-HMQC (c) spectra of the uniformly ^{15}N-labeled Ras protein. In (b) and (c), cross peaks due to Glu^{3} and Glu^{126} are observed.

Sequential assignments

The amide resonances of each residue were related to those of neighbouring residues by using sequential $d_{\alpha N}$ and/or d_{NN} connectivities. For example, in the ^{15}N-edited NOESY spectrum of the Ras protein selectively labeled with [^{15}N]Leu (Fig. 3a), strong NOE cross peaks were observed between the amide protons of L6, L52, L53, L79 and L113 and the $C_{\alpha}H$ protons of the corresponding preceding residues. Further weak intraresidue NOEs were observed between the amide protons and $C^{\alpha}H$ protons of L23, L120, L133, L159 and L168; each of these amide protons also exhibited strong sequential amide-amide NOEs (Fig. 3a). A number of sequential NOEs were also observed for other amino acid residues in ^{15}N-edited NOESY spectra of the selectively ^{15}N-labeled Ras proteins.

Stretches of $d_{\alpha N}$ connectivities

As shown in Fig. 5, strong sequential connectivities ($d_{\alpha N}$) for the T2–G10 stretch were elucidated from analysis of ^{15}N-edited NOESY and TOCSY spectra of the selectively ^{15}N-labeled Ras proteins [and slices of the NOESY-HMQC and TOCSY-HMQC spectra of the Ras protein at δ (^{15}N) = 104.0 ppm for E3]. As for V8 and V9, strips were obtained from the ^{15}N-edited NOESY and TOCSY experiments with a 1–1 echo-type forbidden echo pulse sequence (Fig. 5), because their $C^{\alpha}H$–NH cross peaks were bleached by conventional water resonance suppression. By similar analysis of strong $d_{\alpha N}$ connectivities, seven other stretches (A11–G13, N26–D30, I36–G47, T50–S65, E76–I84, P110–K117, and P140–A146) were identified (data not shown). These connectivities were further confirmed by examination of the 3D TOCSY-HMQC and NOESY-HMQC spectra of the uniformly ^{15}N-labeled Ras protein and the NOESY, DQF-COSY and TOCSY spectra of the Ras protein in $^{1}H_2O$ solution.

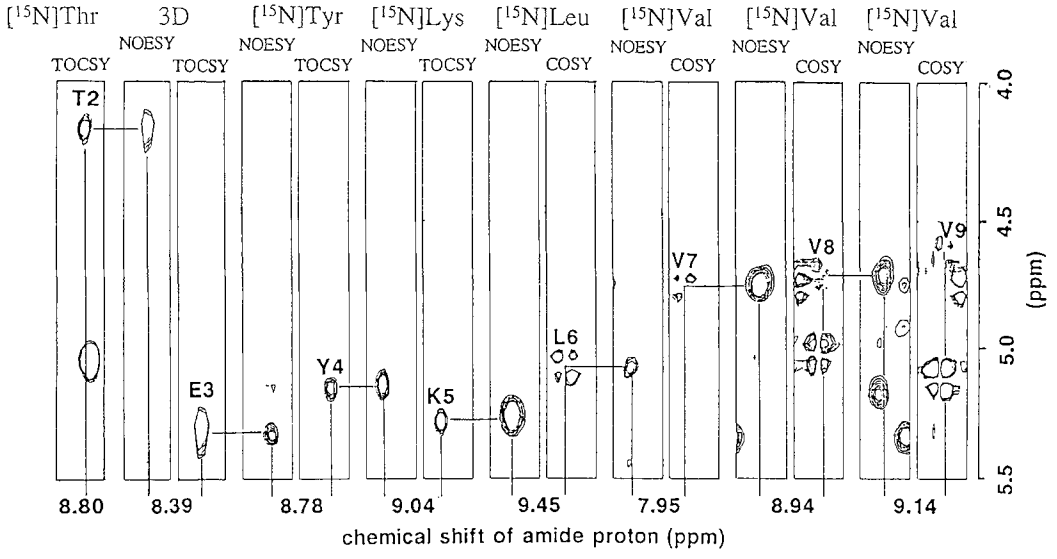

Fig. 5. Connectivities for the T2–V9 stretch in the Ras protein. For E3, strips were collected from 3D NOESY-HMQC and TOCSY-HMQC spectra at $\delta(^{15}N)$ = 104.0 ppm. For other residues, strips were collected from isotope-filtered NOESY, TOCSY and COSY spectra of selectively ^{15}N-labeled samples. For each residue, intraresidue cross peaks appear in TOCSY or COSY spectra and sequential cross peaks appear in NOESY spectra.

Stretches of d_{NN} connectivities

Several d_{NN} connectivities were traced in the 2D HMQC-NOESY spectrum of uniformly ^{15}N-labeled Ras protein. For example, Fig. 6a shows the cross peak assigned to the D105 and S106 sequence. However, the cross peak for the pair, K104 and D105, could not be observed in this experiment, because the ^{1}H chemical shifts were identical (8.05 ppm). The d_{NN} connectivity for K104 and D105 was obtained from the 3D HMQC-NOESY-HMQC experiment (a 3D version of the 2D HMQC-NOESY experiment) because the ^{15}N chemical shifts differed (K104, 92.9 ppm; D105, 96.6 ppm). Thus, in the strip from the 3D HMQC-NOESY-HMQC spectrum at $\delta(^{15}N)$ = 96.6 ppm (Fig. 6b), NOE cross peaks are clearly observed between K104 and D105 as well as between D105 and S106. On the other hand, the 3D NOESY-HMQC spectrum was analyzed to examine the d_{NN} connectivities of amide groups with the same ^{15}N chemical shifts. By combining these 2D and 3D NMR data, all the d_{NN} connectivities of Ras were finally identified. As an example, the d_{NN}-walk along the A18–H27 stretch is shown in Fig. 7. Strong d_{NN} NOEs were found for five other stretches: G13–H27, S65–G77, N85–S106, K117–I139 and S145–L171 (data not shown).

Stretch G10–A11

As described above, the assignment of amide ^{1}H and ^{15}N resonances to T2–G10 and A11–G13 was performed on the basis of $d_{\alpha N}$ connectivities. However, no sequential NOE was found between G10 and A11 in the ^{15}N-edited NOESY spectra of the selectively ^{15}N-labeled Ras protein, probably because selective labeling with [^{15}N]Ala and [^{15}N]Val was not efficient enough.

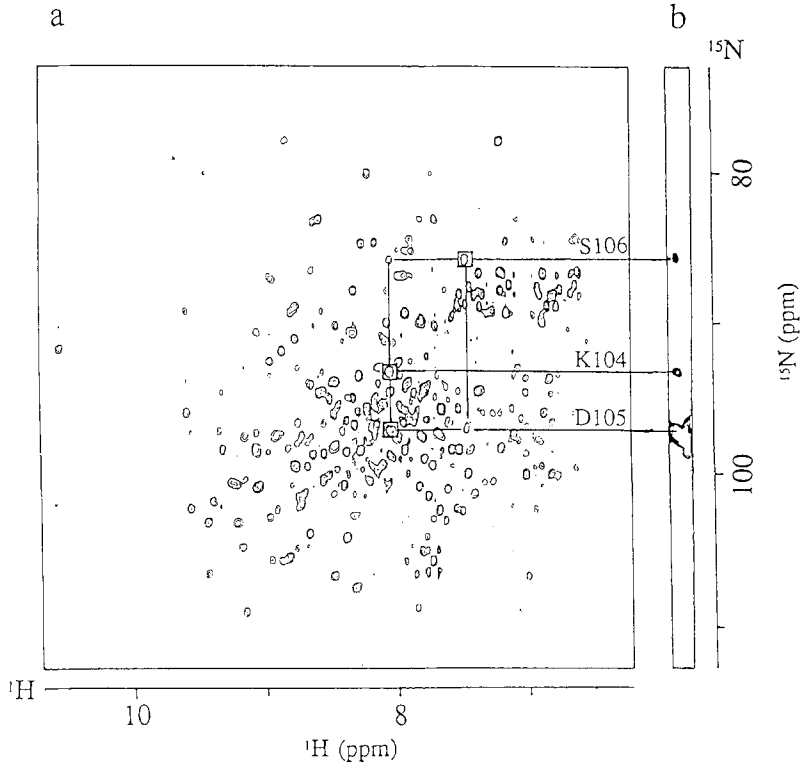

Fig. 6. (a) Amide region of the HMQC-NOESY spectrum (mixing time, 100 ms) of the uniformly ^{15}N-labeled Ras protein. Boxes indicate the intraresidue cross peaks of K104, D105, and S106. Note that the amide ^{1}H chemical shifts of K104 and D105 are the same. (b) Strip from the 3D HMQC-NOESY-HMQC spectrum at δ (^{15}N) = 96.6 ppm; the NOE cross peaks observed for K104–D105 and for D105–S106 are seen.

In contrast, a weak d_{NN} connectivity was unambiguously observed between this pair in the 3D NOESY-HMQC spectrum of the Ras protein that was uniformly ^{15}N-labeled at a high efficiency.

Stretch E31–D33

On the basis of the 3D NOESY-HMQC and TOCSY-HMQC experiments, weak d_{NN} and $d_{\alpha N}$ connectivities were used to assign the amide ^{1}H and ^{15}N resonances of the E31–D33 stretch. In order to confirm the assignments, Y32 of the Ras protein was replaced with F (Phe) by site-directed mutagenesis (Sambrook et al., 1989) and the protein was selectively labeled with [^{15}N]Tyr. All eight ^{1}H–^{15}N cross peaks present in the HSQC spectrum of the Y32F mutant were observed in the HSQC spectrum of the Ras protein selectively labeled with [^{15}N]Tyr. However, the HSQC spectrum of Ras contained an additional cross peak at δ (^{1}H) = 8.71 ppm and δ (^{15}N) = 101.7 ppm. This was accordingly assigned to Y32 (Fig. 8) and confirmed NOE connectivities observed between Y32 and its neighbors E31 and D33.

Stretch S106–V109

Weak d_{NN} connectivities were observed for S106 and D107 in the 2D HSQC-NOESY spectrum

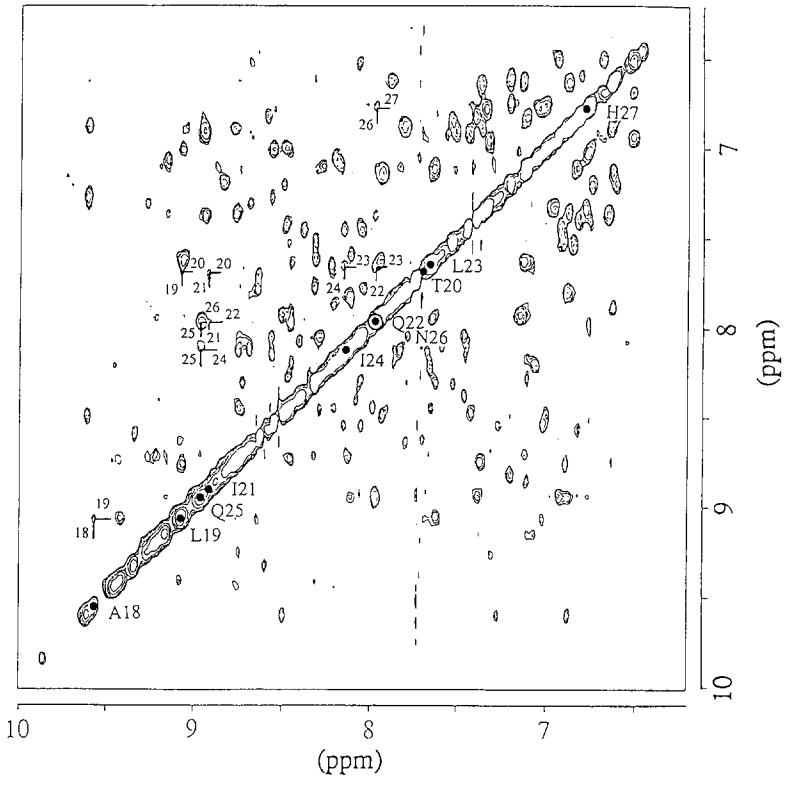

Fig. 7. Amide region of the NOESY spectrum of the Ras protein with a mixing time of 150 ms. The d_{NN} connectivities for the stretch A18–H27 are indicated. Q22 and N26 have the same amide proton chemical shifts.

and for D107 and D108 in the 3D NOESY-HMQC spectrum. Further, a strong $d_{\alpha N}$ connectivity was found for D108 and V109, the unique D–V sequence in the Ras protein. Thus, connectivities were established for the S106–V109 stretch.

Sequential NOEs

In the present study, complete assignment of the backbone ^{1}H and ^{15}N resonances of the Ras protein (except for Pro residues) was achieved by analysis of ^{15}N-edited NOESY and TOCSY spectra together with a variety of 3D NMR spectra. Figure 9 summarizes the observed NOE (d_{NN}, $d_{\alpha N}$, $d_{\beta N}$ and $d_{\alpha N(i,i+3)}$) that provided information for sequential resonance assignments. The assignments of the backbone ^{1}H and ^{15}N resonances are listed in Table 1. Nearly all the C^{α} proton chemical shifts for residues in stretches identified by d_{NN} connectivities were determined from the 3D TOCSY-HMQC spectrum of the uniformly ^{15}N-labeled Ras protein. Those that were not observed in this spectrum, however, were assigned on the basis of their inter- and intraresidue NOEs with other amide protons (Table 1).

Deuterium exchange rates and $^{3}J_{HNH\alpha}$ coupling constants

The deuterium exchange rates of the amide protons were measured to identify secondary

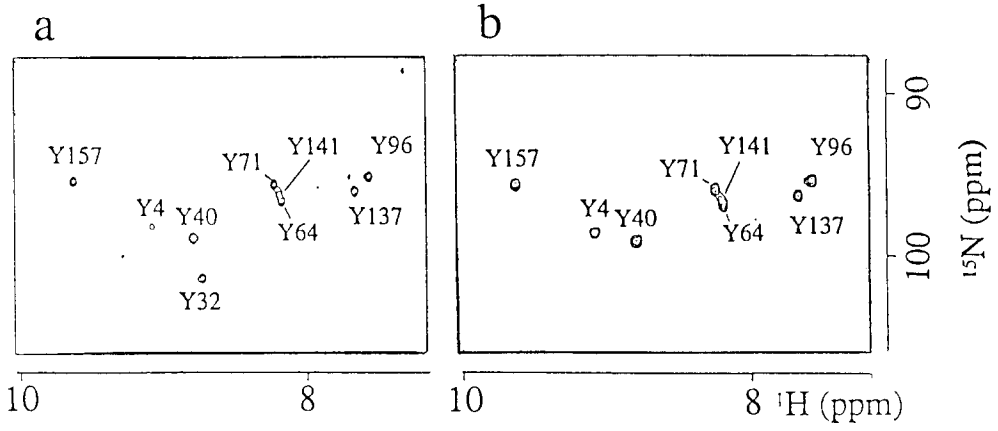

Fig. 8. HSQC spectra of the Ras protein (a) and the Y32F mutant (b), both selectively labeled with [^{15}N]Tyr.

structural elements and their dynamic properties: the lyophilized protein was dissolved in $^{2}H_2O$, and the intensities of ^{15}N–^{1}H cross peaks in the HSQC spectrum were monitored at various times. Thus, a total of 76 amide protons with exchange rates < 0.7 h^{-1} were found (Fig. 9) in addition to seven protons with exchange rates 0.7–2 h^{-1}. Further, in order to locate β strands, vicinal coupling constants, $^{3}J_{HNH\alpha}$, were measured by the HMQC-J experiment (Kay and Bax, 1990). Residues with $^{3}J_{HNH\alpha}$ > 7 Hz were identified as shown in Fig. 9.

α-Helices

Residues involved in α-helices were identified on the basis of strong d_{NN} connectivities and small $^{3}J_{HNH\alpha}$ coupling constants and confirmed by $d_{\alpha N(i,i+3)}$ and $d_{\beta N}$ connectivities (Fig. 9). Thus, five α-helices were found including α1 (S17–I24), α2 (A66–R73), α3 (E91–K104), α4 (E126–Y137), and α5 (V152–L171) as shown in Fig. 9. From observation of slowly exchanging amide protons, helices α1 and α5 were found to be more rigid than the other helices. In contrast, helix α2 was flexible and its amide protons were more accessible to solvent than those in the more rigid helices. These results are consistent with the observed high susceptibility of residues R68–R73 to protease (data not shown).

Topology of β-strands

β-strands and other extended structures in the Ras protein were identified from strong $d_{\alpha N}$ connectivities and large $^{3}J_{HNH\alpha}$ coupling constants. Further, β-strands were distinguished on the basis of slow deuterium exchange rates (Figs. 9 and 10) and interstrand NOEs (Fig. 10). Thus, from extended structures six strands, including β1 (T2–V9), β2 (S39–I46), β3 (E49–D57), β4 (G77–I84), β5 (P110–K117), and β6 (P140–T144), were found to constitute a β-sheet structure with the topology shown in Fig. 10.

The secondary structure of the Ras protein in solution

The secondary structural elements of the GDP-bound Ras protein in aqueous solution determined in the present study are schematically shown in Fig. 11. These structural elements are

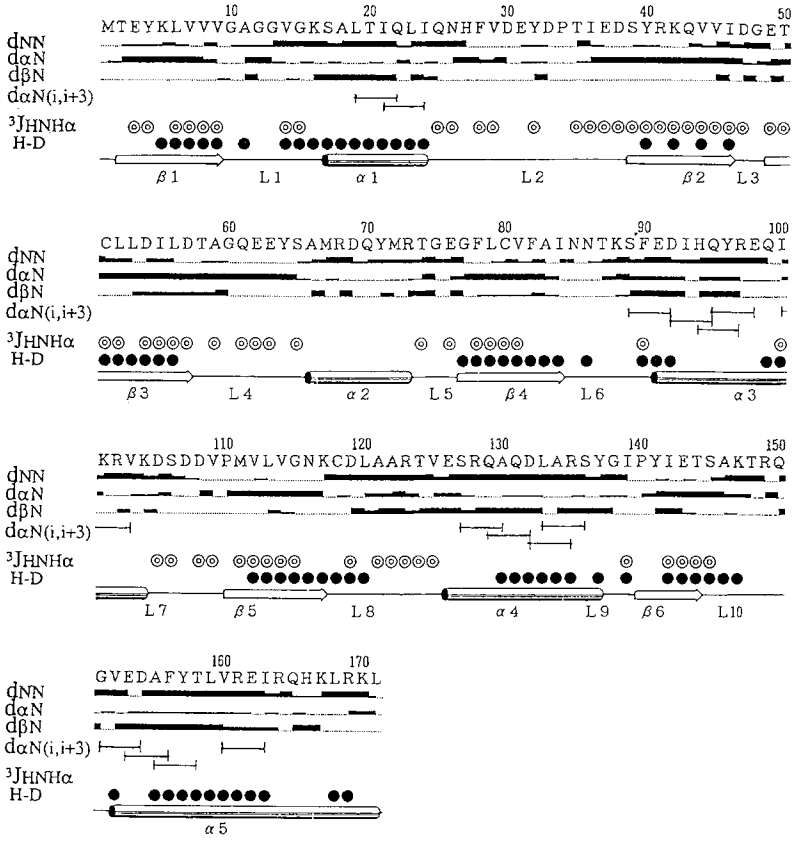

Fig. 9. Summary of NMR information and secondary structure elements of the GDP-bound Ras protein in solution. NOE intensities are indicated by black bars and classified according to the number of contour levels in the 3D NOESY-HMQC spectrum. Double open circles indicate residues with coupling constants $^3J_{HNH\alpha}$>7 Hz. Solid circles indicate backbone amide protons with deuterium exchange rates lower than 0.7 h^{-1} in ^2H_2O solution.

mostly consistent with those found in the crystalline state (de Vos et al., 1988; Tong et al., 1989, 1991). However, we found several interesting features in the secondary and tertiary structure that differed between GDP-bound Ras proteins in solution and in crystal, particularly those related to dynamic structural properties, as discussed below.

X-ray crystallographic studies have identified a β-sheet structure consisting of β1(T2–V9), β2(D38–I46), β3(E49–T58), β4(G77–I84), β5(P110–K117), and β6(P140–T144) (Tong et al., 1991). These β-strands and their topology in the crystalline state agree well with those in solution (Figs. 9–11), except for the dynamic properties of some residues. The X-ray crystallographic study indicated one hydrogen bond between V8 and T58 and two hydrogen bonds between D38 and D57 at one end of the β-sheet (β2:β3:β1) (Tong et al., 1991). NMR analysis confirmed that these three residues are involved in the β-sheet structure, as indicated by an H_α–H_α NOE between S39 and L56 (Yamasaki et al., 1989) and large $^3J_{HNH\alpha}$ values (Fig. 9). However, the amide protons of D38, D57 and T58 exchanged rapidly with solvent water, while other amide protons of the β-sheet exchanged rather slowly (Fig. 9). Therefore, the hydrogen bonds involving D38, D57 and

TABLE 1
^{1}H AND ^{15}N CHEMICAL SHIFTS (PPM) OF BACKBONE RESONANCES OF RAS PROTEIN AT pH 5.5 AND 37°C

Residue	^{15}N	NH	$C^{\alpha}H$	Residue	^{15}N	NH	$C^{\alpha}H$	Residue	^{15}N	NH	$C^{\alpha}H$
Met[1]	*		*	Gln[61]	95.7	8.47	4.45	Ala[121]	99.3	8.10	4.23
Thr[2]	100.2	8.80	4.16	Glu[62]	97.1	8.71	4.26	Ala[122]	98.2	7.57	4.54
Glu[3]	103.9	8.39	5.31	Glu[63]	96.5	8.31	4.27	Arg[123]	96.3	7.93	4.13
Tyr[4]	99.35	8.78	5.11	Tyr[64]	96.9	8.15	4.52	Thr[124]	90.3	9.05	4.57
Lys[5]	100.5	9.04	5.28	Ser[65]	95.4	7.83	4.46	Val[125]	100.6	7.61	4.01
Leu[6]	102.9	9.45	5.07	Ala[66]	104.6	8.66	4.19	Glu[126]	103.6	8.67	4.30
Val[7]	97.3	7.95	4.76	Met[67]	93.6	8.11	4.28	Ser[127]	98.0	9.31	4.05
Val[8]	105.4	8.94	4.72	Arg[68]	96.9	7.82	3.80	Arg[128]	94.3	8.58	4.05
Val[9]	97.2	9.14	4.61	Asp[69]	95.1	8.09	4.29	Gln[129]	93.3	6.83	4.11
Gly[10]	84.3	7.15	3.18,3.49	Gln[70]	94.3	7.87	4.09	Ala[130]	99.7	7.01	3.95
Ala[11]	100.1	9.13	4.50	Tyr[71]	95.8	8.19	4.29	Gln[131]	94.3	8.54	3.76
Gly[12]	82.6	8.56	3.82,4.10	Met[72]	95.1	8.42	4.42	Asp[132]	96.3	8.14	4.45
Gly[13]	91.3	10.55	4.01,4.23	Arg[73]	92.6	7.96	4.00	Leu[133]	99.6	7.46	3.87
Val[14]	89.8	7.70	4.13	Thr[74]	84.8	7.81	4.33	Ala[134]	98.4	8.37	3.80
Gly[15]	86.4	8.62	4.30,4.76	Gly[75]	86.3	7.91	3.38,3.59	Arg[135]	94.6	8.50	4.22
Lys[16]	101.7	10.59	3.53	Glu[76]	97.9	8.81	4.49	Ser[136]	94.0	7.96	4.29
Ser[17]	96.8	9.34	4.28	Gly[77]	77.6	7.19	3.20,4.94	Tyr[137]	96.2	7.62	4.92
Ala[18]	102.0	9.57	3.88	Phe[78]	97.4	8.18	5.45	Gly[138]	87.5	8.31	3.98,4.25
Leu[19]	97.0	9.05	3.86	Leu[79]	103.0	9.19	4.70	Ile[139]	89.6	8.06	5.28
Thr[20]	93.1	7.68	3.45	Cys[80]	100.8	8.70	4.75	Pro[140]	*		*
Ile[21]	97.1	8.90	3.17	Val[81]	102.6	8.96	5.00	Tyr[141]	96.3	8.18	5.98
Gln[22]	97.3	7.96	4.25	Phe[82]	100.3	9.22	4.99	Ile[142]	106.4	8.47	3.95
Leu[23]	96.8	7.67	3.81	Ala[83]	97.7	8.66	5.08	Glu[143]	101.1	7.74	4.83
Ile[24]	90.4	8.09	3.66	Ile[84]	90.1	8.44	4.05	Thr[144]	88.6	8.74	5.05
Gln[25]	92.2	8.94	4.62	Asn[85]	93.4	7.89	5.10	Ser[145]	89.1	8.77	4.91
Asn[26]	93.0	7.97	4.77	Asn[86]	95.4	7.92	5.11	Ala[146]	109.0	9.15	3.91
His[27]	86.6	6.74	4.90	Thr[87]	100.5	9.21	3.85	Lys[147]	92.6	7.08	2.58
Phe[28]	99.3	8.67	5.09	Lys[88]	100.5	8.39	4.19	Thr[148]	82.6	7.69	4.18
Val[29]	101.9	7.55	4.03	Ser[89]	90.8	8.07	4.26	Arg[149]	94.3	7.80	3.48
Asp[30]	98.7	7.78	4.03	Phe[90]	101.0	7.41	4.05	Gln[150]	100.5	7.81	4.11
Glu[31]	95.3	7.65	4.92	Glu[91]	97.9	8.48	3.80	Gly[151]	91.4	8.85	3.82,4.22
Tyr[32]	101.7	8.71	4.31	Asp[92]	93.5	8.45	4.59	Val[152]	96.9	7.10	3.22
Asp[33]	104.8	7.81	4.62	Ile[93]	97.2	7.65	4.02	Glu[153]	93.1	8.28	3.29
Pro[34]	*		*	His[94]	92.5	7.97	4.33	Asp[154]	92.8	8.04	4.23
Thr[35]	86.7	8.93	4.36	Gln[95]	94.2	7.38	3.95	Arg[155]	100.4	8.55	3.76
Ile[36]	97.5	6.92	4.04	Tyr[96]	95.3	7.52	4.09	Phe[156]	88.9	7.26	3.92
Glu[37]	106.9	8.31	4.95	Arg[97]	94.6	8.31	3.68	Tyr[157]	95.6	9.59	4.40
Asp[38]	100.2	8.19	4.82	Glu[98]	93.6	7.75	3.86	Thr[158]	93.6	8.48	3.98
Ser[39]	90.8	8.29	5.55	Gln[99]	96.0	7.89	3.99	Leu[159]	98.0	7.20	3.92
Tyr[40]	98.3	9.04	4.64	Ile[100]	96.1	7.85	3.21	Val[160]	95.3	7.66	3.08
Arg[41]	96.9	8.39	5.85	Lys[101]	94.2	7.78	3.98	Arg[161]	95.4	8.14	3.86
Lys[42]	98.6	8.62	4.50	Arg[102]	94.0	7.77	4.14	Glu[162]	95.6	8.28	4.28
Gln[43]	105.3	8.80	5.32	Val[103]	94.0	8.03	3.91	Ile[163]	99.4	8.44	3.61
Val[44]	97.9	9.05	4.74	Lys[104]	92.9	8.05	4.25	Arg[164]	96.2	8.73	4.05
Val[45]	98.6	8.04	4.65	Asp[105]	96.9	8.05	4.35	Gln[165]	92.6	8.10	4.13
Ile[46]	102.5	8.31	3.99	Ser[106]	85.4	7.47	4.56	His[166]	94.6	8.15	4.35
Asp[47]	106.3	9.42	4.26	Asp[107]	98.3	8.29	4.69	Lys[167]	95.3	8.21	4.19
Gly[48]	79.6	8.19	3.48,4.18	Asp[108]	98.0	8.44	4.85	Leu[168]	95.3	7.65	4.30

TABLE 1 (continued)

Residue	^{15}N	NH	$C^{\alpha}H$	Residue	^{15}N	NH	$C^{\alpha}H$	Residue	^{15}N	NH	$C^{\alpha}H$
Glu^{49}	99.4	7.72	4.63	Val^{109}	98.2	7.52	4.28	Arg^{169}	95.3	7.65	4.29
Thr^{50}	102.1	8.89	4.61	Pro^{110}	*		*	Lys^{170}	98.1	7.94	4.37
Cys^{51}	101.5	9.39	5.18	Met^{111}	99.4	8.13	5.78	Leu^{171}	105.4	7.73	4.21
Leu^{52}	99.1	8.76	4.90	Val^{112}	95.1	8.08	4.33				
Leu^{53}	100.6	9.05	4.92	Leu^{113}	105.4	8.86	5.17				
Asp^{54}	101.1	8.73	5.23	Val^{114}	104.6	9.17	5.10				
Ile^{55}	100.6	9.20	4.71	Gly^{115}	90.9	8.02	2.90,*				
Leu^{56}	104.7	8.76	4.63	Asn^{116}	97.5	8.74	5.58				
Asp^{57}	105.2	8.53	4.81	Lys^{117}	88.6	7.36	4.32				
Thr^{58}	87.1	6.90	4.53	Cys^{118}	90.7	8.75	4.28				
Ala^{59}	98.2	8.97	4.79	Asp^{119}	93.7	8.64	4.50				
Gly^{60}	84.2	8.25	4.14,*	Leu^{120}	97.1	7.79	4.25				

*Not identified.

T58 are not strong, so that this part of the β-sheet structure is flexible. This dynamic feature is not consistent with the rigidity of this region in crystalline states (Tong et al., 1991). This suggests that the salt bridge between D33 of one Ras protein molecule and R135 of another symmetry-related molecule in the crystalline state (Tong et al., 1991) stabilizes the conformation of loop L2 and the end of the antiparallel β-sheet structure. This inherent flexibility of the β-sheet residues in the GDP-bound form may be related to the further distortion of the antiparallel β-sheet structure up to S39 and L56 residues upon ligand exchange from GDP to GTP (Yamasaki et al., 1989). Note that D38 is considered to be involved in the interaction with the target in signal transduction (Adari et al., 1988).

X-ray crystallographic studies have also identified five helices, α1(G15–N26), α2(A66–G75), α3(T87–K104), α4(E126–Y137), and α5(G151–L171) (Tong et al., 1991). The present NMR analysis revealed that helix α1 is shorter than that in the crystalline state, so that Q25 and N26 are not involved in helix but in the loop in the GDP-bound Ras protein in solution. Recently, N26 was found to be essential for the signal transducing activity of Ras (Nur-E-Kamal et al., 1992; Shirouzu et al., 1992). As in the case of D38, this functionally important residue (N26) exhibits a flexible nature in solution. This difference in the dynamic properties between crystal and solution structures may again be ascribed to the intermolecular contact of loop L2 in the crystal structure (Tong et al., 1991). As compared with other α-helices, residues in helix α2 exhibited larger temperature factors in X-ray crystallography (Tong et al., 1991). In agreement with this, helix α2 was found to be the most flexible, while helices α1 and α5 were shown to be as rigid as the β-sheet structure in the GDP bound Ras protein in solution. Although there is a kink in helix α3 at I93 in the crystalline state (Tong et al., 1991), this kink was not found in the present NMR study. However, helix α5 was found to be interrupted at H166 in solution, which was not reported for the crystal structure.

Consistent with the finding that the amide group of A146 is involved in a hydrogen bond with the guanine base (Tong et al., 1991), we also observed that this amide proton undergoes slow solvent exchange in solution. Similarly, the amide protons of G13, G15, K16, and S17 are involved in hydrogen bonds with oxygen atoms of the phosphate groups (Campbell-Burk et al.,

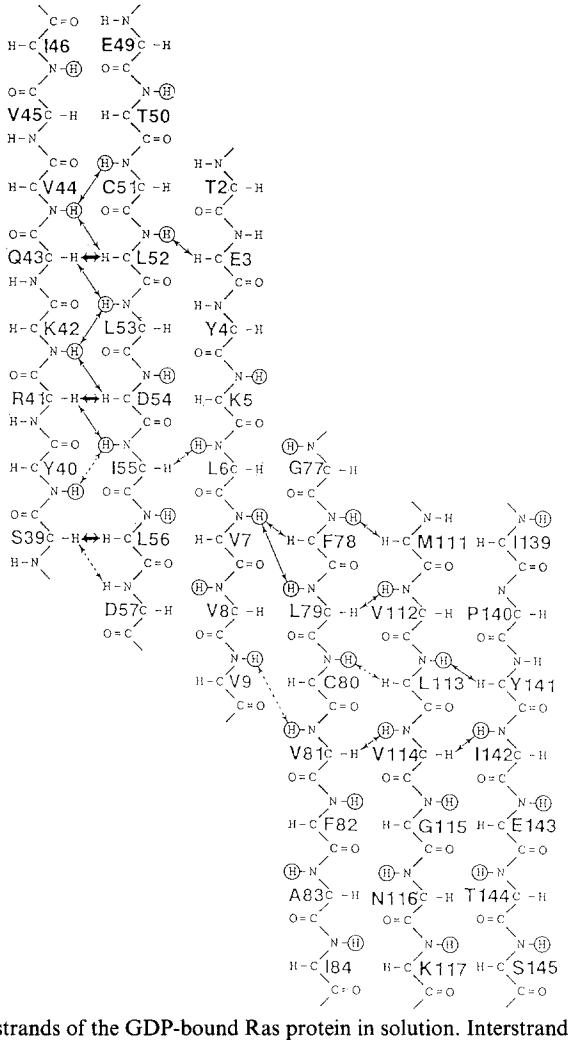

Fig. 10. Topology of the β-strands of the GDP-bound Ras protein in solution. Interstrand NOE intensities are indicated by the corresponding types of arrows. Hydrogen-bonded amide protons are indicated by circles.

1989; Redfield and Papastavros, 1990; Tong et al., 1991) and a type II β-turn is formed between A11 and V14 in the crystalline state (Tong et al., 1991). Thus, these amide protons are slowly exchanged in solution.

In conclusion, all the backbone ^{1}H and ^{15}N resonances (except for Pro residues) of the 171-residue truncated Ras protein were unambiguously assigned in the present study. This complete assignment provides a sound basis for further NMR studies on the GDP-bound Ras protein in solution. First, ^{1}H–^{13}C double resonance and ^{1}H–^{15}N–^{13}C triple resonance experiments (Ikura et al., 1990b-d, 1991; Kay et al., 1990) of the GDP-bound Ras protein are now in progress in our laboratories and should provide side-chain assignments and tertiary structural information. Second, the backbone resonance assignments of the Ras protein will provide a reference for elucidating the effects of mutations on the secondary structure in solution. Third, the interaction of the

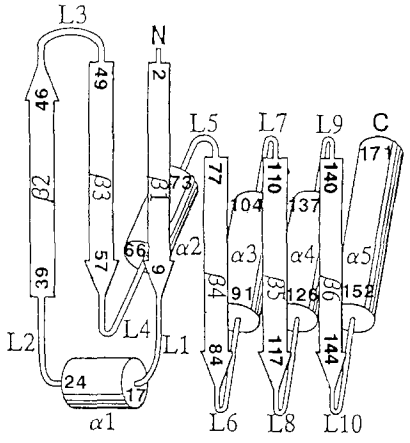

Fig. 11. Secondary structure elements of the GDP-bound Ras protein as determined in the present NMR study. Cylinders indicate α-helices and flat arrows indicate β-strands.

GDP-bound Ras protein with the putative nucleotide-exchange factor (Downward et al., 1990; West et al., 1990; Wolfman and Macara, 1990; Mizuno et al., 1991) can also be analyzed by ^{15}N-edited NMR techniques.

ACKNOWLEDGEMENTS

We are grateful to Dr. B.J. Bachmann of Yale University and Dr. A. Nishimura of the National Institute of Genetics (Mishima, Japan) for the gifts of auxotrophic *E. coli* strains and Dr. G. Kawai of the University of Tokyo for helpful discussions. This work was supported in part by a Grant-in-Aid for Cancer Research from the Ministry of Education, Science, and Culture, Japan and a Grant for 'Biodesign Research Program' from RIKEN, Japan to S.Y.

REFERENCES

Adari, H., Lowy, D.R., Willumsen, B.M., Dar, C.J. and McCormick, F. (1988) *Science*, **240**, 518–521.
Antonny, B., Chardin, P., Roux, M. and Chabre, M. (1991) *Biochemistry*, **30**, 8287–8295.
Bachmann, B.J. (1983) *Microbiol. Rev.*, **47**, 189–230.
Barbacid, M. (1987) *Ann. Rev. Biochem.*, **56**, 779–827.
Bax, A., Griffey, R.H. and Hawkins, B.L. (1983a) *J. Am. Chem. Soc.*, **105**, 7188–7195.
Bax, A., Griffey, R.H. and Hawkins, B.L. (1983b) *J. Magn. Reson.*, **55**, 301–315.
Bax, A. and Davis, G. (1985) *J. Magn. Reson.*, **65**, 355–360.
Bax, A., Sklenar, V., Clore, G.M. and Gronenborn, A.M. (1987) *J. Am. Chem. Soc.*, **109**, 7188–7190.
Bax, A., Clore, G.M., Driscoll, P.C., Gronenborn, A.M., Ikura, M. and Kay, L.E. (1990a) *J. Magn. Reson.*, **87**, 620–627.
Bax, A., Clore, G.M. and Gronenborn, A.M. (1990b) *J. Magn. Reson.*, **88**, 425–431.
Bax, A., Ikura, M., Kay, L.E., Torchia, D.A. and Tschudin, R. (1990c) *J. Magn. Reson.*, **86**, 304–318.
Bax, A. and Ikura, M. (1991) *J. Biomol. NMR*, **1**, 99–104.
Bendall, M.R., Pegg, D.T. and Doddrell, D.M. (1983) *J. Magn. Reson.*, **52**, 81–117.
Bodenhausen, G. and Ruben, D.J. (1980) *Chem. Phys. Lett.*, **69**, 185–189.
Braunschweiler, L. and Ernst, R.R. (1983) *J. Magn. Reson.*, **53**, 521–528.
Brünger, A.T., Milburn, M.V., Tong, L., de Vos, A.M., Jancarik, J., Yamaizumi, Z., Nishimura, S., Ohtsuka, E. and Kim, S.-H. (1990) *Proc. Natl. Acad. Sci. USA*, **87**, 4849–4853.
Campbell-Burk, S. (1989) *Biochemistry*, **28**, 9478–9484.

Campbell-Burk, S., Papastavros, M.Z., McCormick, F. and Redfield, A.G. (1989) *Proc. Natl. Acad. Sci. USA*, **86**, 817–820.
Clore, G.M., Bax, A., Wingfield, P.T. and Gronenborn, A.M. (1988) *FEBS. Lett.*, **238**, 17–21.
Clubb, R.T., Thanabal, V., Osborne, C. and Wagner, G. (1991) *Biochemistry*, **30**, 7718–7730.
Davis, D.G. and Bax, A. (1985) *J. Am. Chem. Soc.*, **107**, 2820–2822.
de Vos, A.M., Tong, L., Milburn, M.V., Matias, P.M., Jancarik, J., Noguchi, S., Nishimura, S., Miura, K., Ohtsuka, E. and Kim, S.-H. (1988) *Science*, **239**, 888–893.
Downward, J., Riehl, R., Wu, L. and Weinberg, R.A. (1990) *Proc. Natl. Acad. Sci. USA*, **87**, 5998–6002.
Driscoll, P.C., Clore, G.M., Beress, L. and Gronenborn, A.M. (1989) *Biochemistry*, **28**, 2178–2187.
Driscoll, P.C., Clore, G.M., Marion, D., Wingfield, P.T. and Gronenborn, A.M. (1990) *Biochemistry*, **29**, 3542–3556.
Fesik, S.W., Gampe Jr., R.T. and Rockway, T.W. (1987) *J. Magn. Reson.*, **74**, 366–371.
Fujita-Yoshigaki, J., Ito, Y., Yamasaki, K., Muto, Y., Miyazawa, T., Nishimura, S. and Yokoyama, S. (1992) *J. Protein Chem*, **11**, 731–739.
Griffey, R.H. and Redfield, A.G. (1987) *Q. Rev. Biophys.*, **19**, 51–82.
Gronenborn, A.M., Bax, A., Wingfield, P.T. and Clore, G.M. (1989) *FEBS. Lett.*, **243**, 93–98.
Ha, J.-M., Ito, Y., Kawai, G., Miyazawa, T., Miura, K., Ohtsuka, E., Noguchi, S., Nishimura, S. and Yokoyama, S. (1989) *Biochemistry*, **28**, 8411–8416.
Hata-Tanaka, A., Kawai, G., Yamasaki, K., Ito, Y., Kajiura, H., Ha, J.-M., Miyazawa, T., Yokoyama, S. and Nishimura, S. (1989) *Biochemistry*, **28**, 9550–9556.
Ikura, M., Bax, A., Clore, G.M. and Gronenborn, A.M. (1990a) *J. Am. Chem. Soc.*, **112**, 9020–9022.
Ikura, M., Kay, L.E. and Bax, A. (1990b) *Biochemistry*, **29**, 4659–4667.
Ikura, M., Kay, L.E., Tschudin, R. and Bax, A. (1990c) *J. Magn. Reson.*, **86**, 204–209.
Ikura, M., Krinks, M., Torchia, D.A. and Bax, A. (1990d) *FEBS Lett.*, **266**, 155–158.
Ikura, M., Kay, L.E., Krinks, M. and Bax, A. (1991) *Biochemistry*, **30**, 5498–5504.
Jeener, J., Meier, B.H., Bachmann, P. and Ernst, R.R. (1979) *J. Chem. Phys.*, **71**, 4546–4553.
John, J., Sohmen, R., Feuerstein, J., Linke, R., Wittinghofer, A. and Goody, R.S. (1990) *Biochemistry*, **29**, 6058–6065.
Kainosho, M. and Tsuji, T. (1982) *Biochemistry*, **21**, 6273–6279.
Kay, L.E., Marion, D. and Bax, A. (1989) *J. Magn. Reson.*, **83**, 72–84.
Kay, L.E. and Bax, A. (1990) *J. Magn. Reson.*, **86**, 110–126.
Krengel, U., Schlichting, I., Scherer, A., Schumann, R., Frech, M., John, J., Kabsch, W., Pai, E.F. and Wittinghofer, A. (1990) *Cell*, **62**, 539–548.
Krontiris, T.G. and Cooper, G.M. (1981) *Proc. Natl. Acad. Sci. USA*, **78**, 1181–1184.
Kumar, A., Ernst, R.R. and Wüthrich, K. (1980) *Biochem. Biophys. Res. Commun.*, **95**, 1–6.
LeMaster, D.M. and Richards, F.M. (1985) *Biochemistry*, **24**, 7263–7268.
LeMaster, D.M. and Richards, F.M. (1988) *Biochemistry*, **27**, 142–150.
Macura, S. and Ernst, R.R. (1980) *Mol. Phys.*, **41**, 95–117.
Marion, D. and Wüthrich, K. (1983) *Biochem. Biophys. Res. Commun.*, **113**, 967–974.
Marion, D., Kay, L.E., Sparks, S.W., Torchia, D.A. and Bax, A. (1989) *J. Am. Chem. Soc.*, **111**, 1515–1517.
McIntosh, L.P. and Dahlquist, F.W. (1990) *Q. Rev. Biophys.*, **23**, 1–38.
McIntosh, L.P., Wand, A.J., Lowry, D.F., Redfield, A.G. and Dahlquist, F.W. (1990) *Biochemistry*, **29**, 6341–6362.
Milburn, M.V., Tong, L., de Vos, A.M., Brünger, A.T., Yamaizumi, Z., Nishimura, S. and Kim, S.-H. (1990) *Science*, **247**, 939–945.
Miller, A.F., Papastavros, M.Z. and Redfield, A.G. (1992) *Biochemistry*, **31**, 10208–10216.
Miura, K., Inoue, Y., Nakamori, H., Iwai, S., Ohtsuka, E., Ikehara, M., Noguchi, S. and Nishimura, S. (1986) *Jpn. J. Cancer Res. (Gann)*, **77**, 45–51.
Mizuno, T., Kaibuchi, K., Yamamoto, T., Kawamura, M., Sakoda, T., Fujioka, H., Matsuura, Y. and Takai, Y. (1991) *Proc. Natl. Acad. Sci. USA*, **88**, 6442–6446.
Muchmore, D.C., McIntosh, L.P. Russel, C.B., Anderson, D.E. and Dahlquist, F.W. (1989) *Methods Enzymol.*, **177**, 44–73.
Müller, L. (1979) *J. Am. Chem. Soc.*, **101**, 4481–4484.
Neal, S.E., Eccleston, J.F. and Webb, M.R. (1990) *Proc. Natl. Acad. Sci. USA*, **87**, 3562–3565.
Nishimura, S. and Sekiya, T. (1987) *Biochem. J.*, **243**, 313–327.

Nur-E-Kamal, M.S.A., Sizeland, A., Abaco, G. and Maruta, H. (1992) *J. Biol. Chem.*, **267**, 1415–1418.
Otting, G., Senn, H., Wagner, G. and Wüthrich, K. (1986) *J. Magn. Reson.*, **70**, 500–505.
Pai, E.F., Kabsch, W., Krengel, U., Holmes, K.C., John, J. and Wittinghofer, A. (1989) *Nature* (London), **341**, 209–214.
Pai, E.F., Krengel, U., Petsko, G.A., Goody, R.S., Kabsch, W. and Wittinghofer, A. (1990) *EMBO J.*, **9**, 2351–2359.
Pelton, J.G., Torchia, D.A., Meadow, N.D., Wong, C.-Y. and Rosenman, S. (1991) *Biochemistry*, **30**, 10043–10057.
Perucho, M., Goldfarb, M., Shimizu, K., Lama, C., Fogh, J. and Wigler, M. (1981) *Cell*, **27**, 467–476.
Pingoud, A., Wehrmann, M., Pieper, U., Gast, F.-U., Urbanke, C., Alves, J., Feuerstein, J. and Wittinghofer, A. (1988) *Biochemistry*, **27**, 4735–4740.
Plateau, P. and Gueron, M. (1982) *J. Am. Chem. Soc.*, **104**, 7310–7311.
Privé, G.G., Milburn, M.V., Tong, L., de Vos, A.M., Yamaizumi, Z., Nishimura, S. and Kim, S-H. (1992) *Proc. Natl. Acad. Sci. USA*, **89**, 3649–3653.
Rance, M., Sørensen, O.W., Bodenhausen, G., Wagner, G., Ernst, R.R. and Wüthrich, K. (1983) *Biochem. Biophys. Res. Commun.*, **117**, 479–485.
Redfield, A.G. and Papastavros, M.Z. (1990) *Biochemistry*, **29**, 3509–3514.
Rensland, H., Lautwein, A., Wittinghofer, A. and Goody, R.S. (1991) *Biochemistry*, **30**, 11181–11185.
Sambrook, J., Fritsh, E.F. and Maniatis, T. (1989) *Molecular Cloning, A Laboratory Mannual*, 2nd Ed., Cold Spring Harbor Laboratory, Cold Spring Harbor, NY.
Satoh, T., Nakamura, S. and Kaziro, Y. (1987) *Mol. Cell. Biol.*, **7**, 4553–4556.
Satoh, T., Endo, M., Nakafuku, M., Akiyama, T., Yamamoto, T. and Kajiro, Y. (1990a) *Proc. Natl. Acad. Sci. USA*, **87**, 7926–7929.
Satoh, T., Endo, M., Nakafuku, M., Nakamura, S. and Kajiro, Y. (1990b) *Proc. Natl. Acad. Sci. USA*, **87**, 5993–5997.
Satoh, T., Nakafuku, M., Miyazima, A. and Kaziro, Y. (1991) *Proc. Natl. Acad. Sci. USA*, **88**, 3314–3318.
Schlichting, I., Wittinghofer, A. and Rösch, P. (1988) *Biochem. Biophys. Res. Commun.*, **150**, 444–448.
Schlichting, I., Almo, S.C., Rapp, G., Wilson, K., Petratos, K., Lentfer, A., Wittinghofer, A., Kabsch, W., Pai, E.F., Petsko, G.A. and Goody, R.S. (1990a) *Nature (London)*, **345**, 309–315.
Schlichting, I., John, J., Frech, M., Chardin, P., Wittinghofer, A., Zimmermann, H. and Rösch, P. (1990b) *Biochemistry*, **29**, 504–511.
Schmidt, J.M. and Rüterjans, H. (1990) *J. Am. Chem. Soc.*, **112**, 1279–1280.
Shaka, A.J. and Freeman, R. (1983) *J. Magn. Reson.*, **51**, 169–173.
Shaka, A.J., Baker, P.D. and Freeman, R. (1985) *J. Magn. Reson.*, **64**, 547–552.
Shih, C., Padhy, L.C., Murray, M. and Weinberg, R.A. (1981) *Nature (London)*, **290**, 261–264.
Shirouzu, M., Fujita-Yoshigaki, J., Ito, Y., Koide, H., Nishimura, S. and Yokoyama, S. (1992) *Oncogene*, **7**, 475–480.
Skelly, J.V., Suter, D.A., Kuroda, R., Neidle, S., Hancock, J.F. and Drake, A. (1990) *FEBS Lett.*, **262**, 127–130.
Stockman, B.J., Krezel, A.M. and Markley, J.L. (1990) *Biochemistry*, **29**, 9600–9609.
Stockman, B.J., Nirmala, N.R., Wagner, G., Delcamp, T.J., DeYarman, M.T. and Freisheim, J.H. (1992) *Biochemistry*, **31**, 218–229.
Tong, L., Milburn, M.V., de Vos, A.M. and Kim, S.-H. (1989) *Science*, **245**, 244.
Tong, L., de Vos, A.M., Milburn, M.V. and Kim, S.-H. (1991) *J. Mol. Biol.*, **217**, 503–516.
Torchia, D.A., Sparks, S.W. and Bax, A. (1988) *Biochemistry*, **27**, 5135–5141.
Torchia, D.A., Sparks, S.W. and Bax, A. (1989) *Biochemistry*, **28**, 5509–5524.
Trahey, M. and McCormick, F. (1987) *Science*, **238**, 542–545.
Valencia, A., Serrano, L., Caballero, R., Anderson, P.S. and Lacal, J.C. (1988) *Eur. J. Biochem.*, **174**, 621–627.
West, M., Kung, H.-F. and Kamata, T. (1990) *FEBS Lett.*, **259**, 245–248.
Wolfman, A. and Macara, L.G. (1990) *Science*, **248**, 67–69.
Wüthrich, K., Billeter, M. and Braun, W. (1984) *J. Mol. Biol.*, **180**, 715–740.
Wüthrich, K. (1986) *NMR of Proteins and Nucleic Acids*, Wiley-Interscience, New York.
Yamasaki, K., Kawai, G., Ito, Y., Muto, Y., Fujita, J., Miyazawa, T., Nishimura, S. and Yokoyama, S. (1989) *Biochem. Biophys. Res. Commun.*, **162**, 1054–1062.
Yamasaki, K., Muto, Y., Ito, Y., Wälchli, M., Miyazawa, T., Nishimura, S. and Yokoyama, S. (1992) *J. Biomol. NMR*, **2**, 71–82.
Zuiderweg, E.R.P. and Fesik, S.W. (1989) *Biochemistry*, **28**, 2387–2391.